

A comparison between the probabilistic and possibilistic approaches: the importance of a correct metrological information

Alessandro Ferrero, *Fellow, IEEE*, and Simona Salicone, *Senior Member, IEEE*

Abstract—When dealing with measurement uncertainty, a metrologist is required to take into consideration many different points. The most important ones are: the uncertainty contributions affecting the measurement process; the random or systematic nature of these contributions; the available metrological information about these contributions. Last, but not less important, the particular measurement process itself.

This paper shows, with two simple examples, the importance of correctly considering all aforementioned points in evaluating uncertainty. The GUM approach, a Monte Carlo approach, sometimes different from the one recommended by the GUM Supplement 1, and the RFV approach are compared, proving that the RFV approach leads to the simplest and most straightforward way to consider all these points.

Index Terms—Measurement uncertainty; Possibility theory; Random contributions; Random-Fuzzy Variables; Systematic contributions; GUM; Monte Carlo.

I. INTRODUCTION

Nowadays, the scientific community has widely accepted that a measurement result is meaningless if not associated to an uncertainty value. On the other hand, the mathematical framework within which uncertainty can be better evaluated is still under discussion. The present standards [1], [2] refer to probabilistic approaches, while the research of the last 15 years has also focused on possibilistic approaches [3]–[20].

No matter on the followed approach, an incorrect consideration of the available metrological information may lead to the incorrect assumption that similar uncertainty contributions should be always processed in the same mathematical way. Indeed, the nature of the considered contributions does not indicate, alone, how they must be combined, because the measurement process may have a significant impact on the way they propagate. In other words, the same uncertainty contributions might lead to very different results when the measurement procedure is even slightly modified. This is particularly important when systematic and unknown systematic contributions affect the measurement procedure, as widely discussed in the literature covering different applications [21]–[24]. Moreover, the correct exploitation of the available metrological information becomes even more important when the possibilistic approach is considered, which implies the application of different mathematical operators, according to

the different assumptions, thus yielding a high effectiveness in handling the available metrological information.

In this paper, a simple example is considered under different metrological assumptions, to show how different interpretations of the available metrological information may have a significant impact on the obtained uncertainty value under both the probabilistic and possibilistic approaches. The example is intentionally chosen to be very simple, maybe also trivial, so that the Readers do not need to concentrate on complicated algorithms and can fully focus on the method and the obtained results. The aim is to reaffirm the central role of each available piece of metrological information in the evaluation of uncertainty on the final measurement result. Furthermore, the RFV approach in the possibilistic framework and the application of the related mathematics [3], [5], [7] are reconsidered in this paper, to give a clearer perspective on their use, when different applications are considered.

II. THE MATHEMATICAL BACKGROUND

In this section, the probabilistic and possibilistic approaches to the evaluation and propagation of the measurement uncertainty are briefly recalled.

A. The probabilistic approach

Let us consider the measurement function $Y = f(X_1, X_2, \dots, X_N)$, that links the desired physical quantity Y to the measured physical quantities X_1, X_2, \dots, X_N .

The main assumption underlying the probabilistic approach is that all significant systematic effects affecting the measurement process have been recognized and proper compensations applied.

1) *The GUM approach*: The fundamental standard document, when dealing with measurement uncertainties, is represented by the *Guide to the Expression of Uncertainty in Measurement* (GUM) [1].

According to the suggestions of the GUM, it is possible to obtain the best estimates x_k of every input quantity X_k (with $k = 1 \dots N$) and the best estimate $u(x_k)$ of the associated measurement uncertainty [1]. Then, it is possible to evaluate the best estimate of the output quantity Y as [1]:

$$y = f(x_1, x_2, \dots, x_N) \quad (1)$$

The authors are with the Department of Electronics, Information and Bioengineering (DEIB), Politecnico di Milano, p.za Leonardo da Vinci 32, I-20133 Milano, Italy (e-mail: alessandro.ferrero@polimi.it, simona.salicone@polimi.it).

and its associated standard uncertainty $u_c(y)$, called combined standard uncertainty, as [1]:

$$u_c(y)^2 = \sum_{i=1}^N \left(\frac{df}{dx_i} \right)^2 u^2(x_i) + 2 \sum_{i=1}^{N-1} \sum_{j=i+1}^N \frac{df}{dx_i} \frac{df}{dx_j} \rho(x_i, x_j) u(x_i) u(x_j) \quad (2)$$

Eq. (2) is known as the law of propagation of standard uncertainties (LPU) and is derived by the first-order Taylor series approximation of the measurement function f [1]. In (2): $\frac{\partial f}{\partial x_i}$, called *sensitivity coefficients*, are the partial derivatives of function f with respect to quantities x_i , evaluated in x_1, x_2, \dots, x_n ; $u(x_i)$ is the standard uncertainty associated to quantity x_i ; $\rho(x_i, x_j)$ is the estimated correlation coefficient between x_i and x_j , which satisfies the following properties: $-1 \leq \rho(x_i, x_j) \leq 1$, $\rho(x_i, x_j) = \rho(x_j, x_i)$ and $\rho(x_i, x_j) = 0$ when quantities x_i and x_j are uncorrelated.

According to the GUM [1], $u_c(y)$ is the quantity that correctly characterizes the dispersion of the values that could reasonably be attributed to measurand Y . Given a coverage probability p , the associated confidence interval, or coverage interval, is an interval centered on y , with semi-width $k_p u_c(y)$, where k_p is the evaluated coverage factor [1]:

$$Y_p = [y - k_p u_c(y), y + k_p u_c(y)] \quad (3)$$

While $u_c(y)$ does always represent, by definition, the positive square root of the second moment of the probability distribution (PDF) associated to the values that can reasonably be attributed to measurand Y , the correct evaluation of the coverage factor k_p depends on the exact knowledge of this PDF and is correct only to the extent the assumptions made on this PDF are valid [1]. A general practice, when this PDF is not known, is to apply the *Central Limit Theorem* and to use the k_p values typical of a normal PDF.

2) *The Monte Carlo approach*: Whenever the assumptions behind the LPU are not satisfied, the *Supplement 1 to the Guide to the Expression of Uncertainty in Measurement – Propagation of distributions using a Monte Carlo method* (GUM1) [2] recommends a numerical approach, which is perfectly consistent with the broad principles of the GUM [2].

The approach is simply based on Monte Carlo simulations and allows one to obtain the histogram which approximates the PDF associated to the final measurement result Y , starting from the PDFs associated to the input quantities X_1, X_2, \dots, X_N .

A correct application of the Monte Carlo method, by providing an estimate of the final PDF of the values that can reasonably be attributed to the measurand, overcomes the limitations on the evaluation of the coverage probability assigned to interval Y_p defined by the expanded uncertainty.

B. The possibilistic approach

In this section, the possibilistic approach based on the Random-Fuzzy variables (RFVs) is recalled.

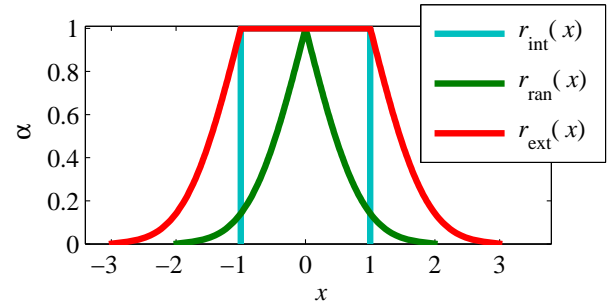


Fig. 1. Example of RFV (red + cyan lines) and its PDs: $r_X^{\text{int}}(x)$ (cyan line), $r_X^{\text{ran}}(x)$ (green line), $r_X^{\text{ext}}(x)$ (red line).

RFVs are type-2 fuzzy variables [25], suitably defined to represent a measurement result together with its uncertainty [26]. Fig. 1 shows an example of RFV, together with the possibility distributions (PDs) from which it is defined [26]: the “internal PD” $r_X^{\text{int}}(x)$ represents the systematic and unknown contributions to uncertainty affecting the measurement result and the “external PD” $r_X^{\text{ext}}(x)$ represents all contributions to uncertainty. This last PD is obtained by combining $r_X^{\text{int}}(x)$ with the “random PD” $r_X^{\text{ran}}(x)$, which represents only the random contributions to uncertainty, as [26], [27]:

$$r_X^{\text{ext}}(x) = \sup_{x'} T_{\min} [r_X^{\text{ran}}(x - x' + x^*), r_X^{\text{int}}(x')] \quad (4)$$

where x^* is the mode of r_X^{ran} and $T_{\min}(a, b) = \min(a, b)$ is a fuzzy operator, belonging to the class of t -norm operators, called *min t-norm* [25].

Both the internal and random PDs can be built starting from the available metrological information, as shown in [10], [26]. In general, the information on the random contributions to uncertainty is available in terms of PDFs. Therefore, in such situations, the random PD is derived by applying suitable probability-possibility transformations to the given PDF [6], [26], [28]. On the other hand, the information about the systematic contributions is not always given in terms of PDFs. Very often only an interval of variation of the contribution is given. For instance, in all data sheets and calibration certificates, an accuracy interval is given, around the measured value. This situation is called by Shafer [29] *total ignorance* and can be represented by a rectangular PD $r_X^{\text{int}}(x)$ over the given interval [26].

The cuts of a PD are called α -cuts. α denotes the cut level and, because of the normalization condition of PDs, it is always $0 \leq \alpha \leq 1$. It is immediate to associate a degree of belief to each α -cut. In particular, the one associated to the α -cut at level α is $1 - \alpha$ [26]. It can be proved [9] that the α -cuts of a PD extend, to the possibility theory, the probabilistic concept of coverage intervals. Therefore, in the following, the term “coverage interval” will be used for the sake of simplicity in both the probabilistic and possibilistic frameworks. Furthermore, in the possibilistic framework, the concept of degree of belief extends the probabilistic concept of coverage probability. Therefore, when PDs are considered to represent measurement results, it is straightforward to obtain the coverage intervals and associated degrees of belief; as an

example, the α -cut at level 0.05 is the coverage interval with a 95% degree of belief, associated to the measured value.

When an RFV is considered, the α -cuts of $r_X^{\text{ext}}(x)$ provide the coverage intervals associated with the measurement result due to all contributions to uncertainty, while the α -cuts of $r_X^{\text{int}}(x)$ provide the coverage intervals due only to the systematic effects. Therefore, for each degree of belief (corresponding to the coverage probability in the probability framework), it is known how the random and systematic contributions affect the final measurement result [9], [15], [18], [26].

Let us now consider the measurement model $z = f(x, y)$, which corresponds, in the possibility domain, to the evaluation of the RFV associated to the final measurement result¹ z , given the RFVs associated to x and y .

A general rule to perform the combination of PDs is Zadeh's extension principle (ZEP) [31], defined by:

$$r_Z(z) = \sup_{z=f(x,y)} (r_{X,Y}(x,y)) \quad (5)$$

where $r_{X,Y}(x,y)$ is the joint possibility distribution (JPD) of x and y . Of course, since an RFV is composed by two PDs, (5) has to be applied twice: when the internal JPD $r_{X,Y}^{\text{int}}(x,y)$ is considered, the internal PD $r_Z^{\text{int}}(z)$ is obtained; similarly, when the external JPD $r_{X,Y}^{\text{ext}}(x,y)$ is considered, the external PD $r_Z^{\text{ext}}(z)$ is obtained.

Within the possibility theory, the JPD is defined through a family of mathematical operators, called t -norms [32]. In particular, when X and Y are independent variables, the JPD is defined as:

$$r_{X,Y}(x,y) = T(r_X(x), r_Y(y)) \quad (6)$$

On the other hand, when X and Y are not independent, the JPD is defined as:

$$r_{X,Y}(x,y) = T(r_X(x), r_{Y|X}(y|x)) = T(r_{X|Y}(x|y), r_Y(y)) \quad (7)$$

where $r_{Y|X}(y|x)$ and $r_{X|Y}(x|y)$ are the conditional PDs of Y , given X , and X , given Y , respectively [5], [7]. It can be proved [5], [7] that the conditional PDs are derived in such a way to keep into account the dependence of X on Y and viceversa, thus encompassing the role played by correlation in the probability framework.

Eqs. (6) and (7) show that the JPD is not defined in an univocal way but, starting from the same variables, different JPDs are obtained when different t -norms are applied. As discussed in [5], [7], the choice of the t -norm to be employed in (6), or (7), is a crucial point in the combination of RFVs.

In the literature, many different t -norms are defined. A very simple t -norm, already mentioned above, is the *min* t -norm T_{\min} . Another t -norm is, for example, the Frank parametric family of t -norms [32]:

$$T_\gamma^F(a,b) = \begin{cases} T_{\min}(a,b) = \min(a,b) & \text{if } \gamma = 0 \\ T_{\text{prod}}(a,b) = a \cdot b & \text{if } \gamma = 1 \\ T_L(a,b) = \max(0, a+b-1) & \text{if } \gamma = \infty \\ \log_\gamma \left(1 + \frac{(\gamma^a - 1) \cdot (\gamma^b - 1)}{\gamma - 1} \right) & \text{otherwise} \end{cases} \quad (8)$$

¹The following results, derived, for the sake of simplicity, in the simple case of a function of two variables, can be readily extended to the most general case, because of the associative property of the employed t -norms [30].

whose behavior depends on the choice of the parameter γ . Other t -norms depend on two parameters, as, for instance, the generalized Dombi t -norm [32], [33].

When different t -norms are applied, different JPDs are obtained. Similarly, when a parametric family of t -norms is considered, different JPDs are obtained, according to the chosen value of the parameters [5], [33]. In any case, regardless to the employed t -norm, the JPD is always obtained in closed form.

It has been shown that, when PDs are used to model measurement results and the associated uncertainty, the application of the Frank t -norm to process these PDs provides a good estimation of the way the different uncertainty contributions combine [5], [33]. Hence, as an example, let us see what happens when two PDs are considered and combined to build a joint PD, when different γ values in (8) are considered.

Let us consider Figs. 2 and 3, where different t -norms are applied to the same PDs r_X and r_Y , which are considered independent, for the sake of simplicity. In particular, the *min* t -norm is applied (the *min* t -norm is a particular Frank t -norm, for $\gamma = 0$) in Fig. 2, while the Frank t -norm $T_{\gamma=0.1}^F$ is applied in Fig. 3.

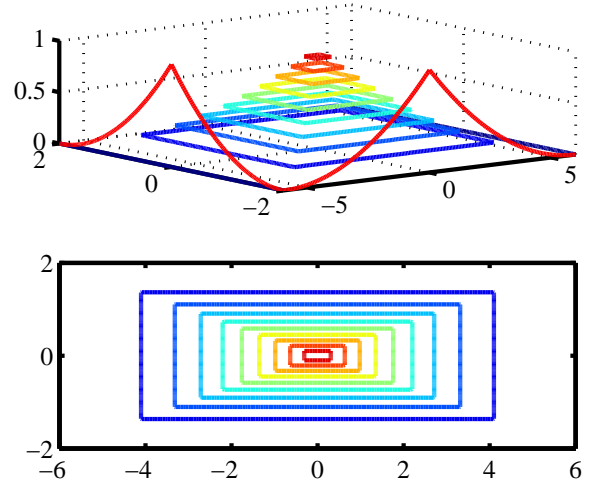


Fig. 2. Joint PD $r_{X,Y}$ of independent PDs r_X and r_Y obtained with $T_{\gamma=0}^F = T_{\min}$ (upper plot) and its α -cuts (bottom plot).

The bottom plot of Fig. 2 shows rectangular 2D α -cuts of the obtained JPD, while the bottom plot of Fig. 3 shows that the 2D α -cuts of the obtained JPD show an ellipsoidal shape. This is a general result and does not depend on the considered initial PDs. Furthermore, for every value α , the ellipsoidal shape is included into the rectangle, thus suggesting that the rectangle considers all possible combinations of the values of the initial PDs, while, in the ellipsoidal shape, a compensation is considered, that tends to exclude, among all possible pairs of values, those obtained by combining the values closer to the edges of the initial PDs.

Therefore, when a Frank t -norm is applied, the optimal choice of T in (6) and (7) translates into the optimal choice of γ in (8). In particular, as proved in [5], [7]:

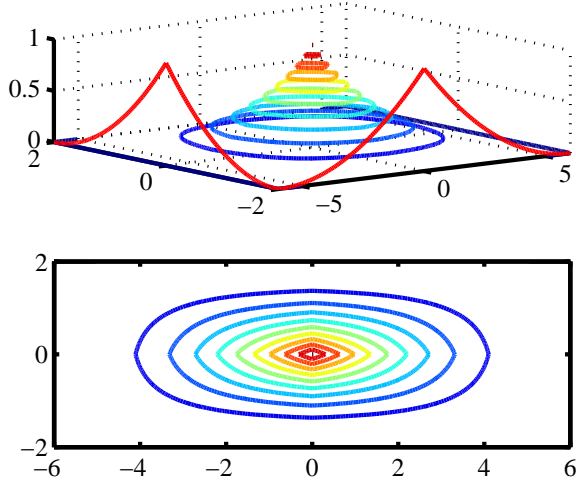


Fig. 3. Joint PD $r_{X,Y}$ of independent PDs r_X and r_Y obtained with $T_{\gamma=0.1}^F$ (upper plot) and its α -cuts (bottom plot).

- the value $\gamma = 0$ (which corresponds to the application of the *min t*-norm T_{min}) is the optimal one when the available information shows that the PDs do not represent random phenomena and their combination does not imply any probabilistic inference;
- a value $0 < \gamma \leq 1$ must be used when the available information shows that the PDs represent random phenomena or when their combination implies a probabilistic inference. In particular, it was proved that: $\gamma = 1$ (which corresponds to the application of the *product t*-norm T_{prod}) is the optimal value when the PDs are triangular (representing, in the possibility domain, uniform probability distributions); $\gamma = 0.05$ is the optimal value when the PDs represent, in the possibility domain, normal probability distributions; $\gamma = 0.1$ is the optimal value for all other PD shapes.

The above considerations lead to conclude that, when two RFVs shall be combined, their random JPD $r_{X,Y}^{ran}(x,y)$ is always obtained by applying a Frank *t*-norm with $0 < \gamma \leq 1$, since the combination of random contributions does always imply a probabilistic inference. On the other hand, since the combination of the non random contributions may, or may not, imply a probabilistic inference, according to the considered measurement procedure, as it will be shown in the following examples, the internal JPD $r_{X,Y}^{int}(x,y)$ can be obtained by applying either the *min t*-norm T_{min} or a Frank *t*-norm T_{γ}^F with $0 < \gamma \leq 1$.

After having built the two JPDs $r_{X,Y}^{int}(x,y)$ and $r_{X,Y}^{ran}(x,y)$, the ZEP (5) must be applied to obtain the RFV of the final measurement result Z . In particular, when the measurement function f is linear, according to the law of superposition of the effects²:

²From the practical point of view, this simpler approach, which is theoretically valid only for linear functions, can be also followed when function f is approximately linear in the neighborhood of the measured value, specified by the uncertainty value.

- 1) $r_Z^{int}(z)$ is obtained starting from $r_{X,Y}^{int}(x,y)$;
- 2) $r_Z^{ran}(z)$ is obtained starting from $r_{X,Y}^{ran}(x,y)$;
- 3) $r_Z^{ext}(z)$ is evaluated from (4).

In the more general case, when function f is non linear, it is not possible to apply the superposition principle and therefore it is necessary to apply the ZEP on $r_{X,Y}^{int}(x,y)$ and on the external JPD [3]:

$$\begin{aligned} r_{X,Y}^{ext}(x,y) &= \\ &= \sup_{x',y'} T_{min} [r_{X,Y}^{ran}(x-x'+x', y-y'+y'), r_{X,Y}^{int}(x',y')] \end{aligned} \quad (9)$$

where (x^*, y^*) is the mode of $r_{X,Y}^{ran}$. It can be readily seen that (9) is an extension of (4).

III. EXAMPLES

The considered examples are related to the possible situations that can be met in measuring length and width of a small rectangular block by means of a Vernier caliper with 0.05 mm resolution. This is such a typical situation in many industrial applications, that it may be proposed as an exercise in technical schools to fully understand all possible implications when evaluating uncertainty. Therefore, for the sake of clarity and generality, the example is here proposed as an exercise, assigned to a class of a technical school.

A. The assumptions

The block under test is first measured by the instructor, using a comparator and a set of Johansson gauge blocks, so that the measured values can be considered as reference values. The following values are supposed to be measured for length l and width w respectively: $l_{ref} = 77.32$ mm and $w_{ref} = 21.18$ mm.

All students in the class are then requested to calibrate their own calipers against the Johansson gauge blocks, in the range of the dimensions of the block under test. The deviations between the gauge block nominal values and the values measured by the calipers represent the systematic contributions to uncertainty introduced by the different calipers. The distribution of all obtained deviations is then considered and found to be uniform over interval ± 0.1 mm.

A random contribution to uncertainty, mainly due to reading errors, is also considered, and, for the sake of simplicity in the following computations, it is assumed to distribute uniformly over the ± 0.05 mm interval.

B. The considered experiments

The experiments that will be considered have been designed to reproduce some typical industrial situations related to the way the available metrological information is exploited. The first situation assumes that the measured values are corrected using the calibration data related to the specific caliper employed to perform the measurement. The second situation assumes that the measured values are not corrected, but that the distribution of the systematic contributions is considered in evaluating uncertainty. At last, a third situation is considered,

where the only information available to take into account the systematic effects in uncertainty evaluation is their interval of variations, with no information about the distribution.

According to the above assumptions, the following experiments are considered.

1) *Length and width measurements*: The students are requested to evaluate the measurement uncertainty on the measured values of length and width of the block under test, under the three considered situations, for which the available information is summarized in Table I.

In case 1A, the two quantities are measured with one (or two) specific caliper(s), and the systematic error affecting the measured values is compensated. On the other hand, in both cases 2A and 3A, the two quantities are measured with one (or two) caliper(s), randomly taken among all student's calipers. This way, it is not known which caliper is used and which is the specific systematic error it introduces, so that it is not possible to compensate for it. Furthermore, in case 2A, it is supposed to know the distribution of the systematic errors over the given interval, while, in case 3A, it is supposed to know only the interval of variation.

The considered measured values of length and width are denoted l_m and w_m respectively. In particular:

- *Case 1A*. When only one caliper is used to measure both length and width, it is supposed to introduce a systematic error $e_{sys}^l = e_{sys}^w = -0.06$ mm, and the measured values are supposed to be $l_m = 77.25$ mm and $w_m = 21.10$ mm. On the other hand, when two different calipers are used, it is supposed that the caliper used to measure the length introduces a systematic error $e_{sys}^l = -0.06$ mm and that the measured value is $l_m = 77.25$ mm; while it is supposed that the caliper used to measure the width introduces a systematic error $e_{sys}^w = 0.03$ mm and that the measured value is $w_m = 21.20$ mm.
- *Case 2A and Case 3A*. For these cases, we suppose that the two measurements are taken with the same caliper. Therefore, the considered measured values of length and width are $l_m = 77.25$ mm and $w_m = 21.10$ mm, respectively.

2) *Area measurement*: The students are required to evaluate the measurement uncertainty on the area of the surface of the block under test, evaluated starting from the measured length and width values and uncertainty values. Therefore, from the above three measurement conditions (Table I), five different measurement conditions are now derived, as summarized in Table II.

The area reference value is given by³ $A_{ref} = l_{ref} \cdot w_{ref} = 1637.6$ mm², while the considered measured value of the area depends on the considered case, according to the previous example. In particular:

- *Case 1B*. When the systematic error introduced by the caliper(s) is known, it is possible to compensate for it. Hence, the area can be obtained as:

$$A_m = (l_m - e_{sys}^l) \cdot (w_m - e_{sys}^w)$$

³This area value and the following ones are given with one decimal digit. Of course, the number of significant digits is related to the uncertainty values that will be evaluated in the following sections.

When only one caliper is used to measure both length and width, the two measured values are corrected for the same systematic error $e_{sys}^l = e_{sys}^w = -0.06$ mm (according to the above assumptions), thus obtaining $A_m = 1635.9$ mm². When two calipers are used, the length is corrected for error $e_{sys}^l = -0.06$ mm while the width is corrected for error $e_{sys}^w = 0.03$ mm (according to the above assumptions). Hence, it follows $A_m = 1636.7$ mm².

- *Case 2B, 3B, 4B, 5B*. When the systematic error introduced by the caliper(s) is not known, it is not possible to make any compensation. Therefore, the value of the area is simply obtained as:

$$A_m = l_m \cdot w_m$$

According to the above assumptions, $l_m = 77.25$ mm and $w_m = 21.10$ mm are considered for all cases, so that the measured value is the same in all cases and the obtained probability and possibility distributions are centered on the same mode, thus making the comparison more evident. Under this assumption, it follows $A_m = 1629.9$ mm².

3) *Uncertainty evaluation*: For each considered case, three approaches are followed and then the obtained results compared: the application of the GUM probabilistic approach [1], which defines the uncertainty value as the standard deviation of the considered probability distribution and then combines uncertainties through the LPU (in the following, *GUM approach*); the application of the Monte Carlo method, which considers the entire probability distributions and combine them through Monte Carlo simulations (in the following, *MC approach*); the application of the possibilistic approach, as described in Sec. II-B (in the following, *RFV approach*).

It is worth noting that the Monte Carlo method considered in the following is different from the one suggested by the Supplement 1 to the GUM [2], when systematic errors are involved. Indeed, Supplement 1, in a very similar example as the one considered here, recommends to extract a new value of the systematic error at each iteration. This approach (that has been already challenged in the literature [21], and also by authors that follow the theoretical approach considered by the GUM and its Supplement 1 [24]) appears to be not fully consistent with the need to exploit all available metrological information when evaluating uncertainty [23]. In the considered case, the available information shows that the systematic error, though unknown, affects all measurements in the same way. Therefore, a different procedure will be proposed and employed in the following examples.

It will be shown how the considered example, though quite simple, yields a significant comparison of the three considered approaches, giving evidence that the RFV one is the most versatile in taking into account the available relevant metrological information.

IV. CASE A RESULTS

A. Case 1A

In case 1A, since the calipers are known and the systematic errors are compensated, only random, uniformly distributed,

TABLE I
SCHOOL WORK A: AVAILABLE METROLOGICAL INFORMATION IN THE THREE DIFFERENT CONSIDERED CASES.

	RANDOM	SYSTEMATIC
case 1A	uniform PDF (width ± 0.05 mm)	compensated
case 2A	uniform PDF (width ± 0.05 mm)	uniform PDF (width ± 0.1 mm)
case 3A	uniform PDF (width ± 0.05 mm)	interval (width ± 0.1 mm)

TABLE II
SCHOOL WORK B: AVAILABLE METROLOGICAL INFORMATION IN THE FIVE DIFFERENT CONSIDERED CASES.

case	procedure	RANDOM	SYSTEMATIC
1B	known caliper(s)	uniform PDF (width ± 0.05 mm)	compensated
2B	1 unknown caliper	uniform PDF (width ± 0.05 mm)	uniform PDF (width ± 0.1 mm)
3B	2 unknown calipers	uniform PDF (width ± 0.05 mm)	uniform PDF (width ± 0.1 mm)
4B	1 unknown caliper	uniform PDF (width ± 0.05 mm)	interval (width ± 0.1 mm)
5B	2 unknown calipers	uniform PDF (width ± 0.05 mm)	interval (width ± 0.1 mm)

contributions are present. In this case, since only random contributions, with known PDF, are present, the GUM approach can provide the correct coverage intervals of length and width, at given coverage probabilities. The other two approaches are nevertheless considered, for a comparison.

Let us then first consider the GUM approach. For uniform distributions, the coverage intervals can be readily obtained. In fact, given an uniform PDF over interval I , the coverage interval corresponding to the coverage probability p (with $0 \leq p \leq 1$) is a fraction p of I , centered on the same mean value as that of I . Hence, according to the assumptions summarized in Table I, the GUM approach provides, for this case 1A, intervals of width $0.05 \cdot p$ mm, centered on values $l_m - e_{sys}^l$ and $w_m - e_{sys}^w$, respectively, for length and width, where the values of e_{sys}^l and e_{sys}^w are the ones given in sec. III-B1.

When the MC approach is followed, that in this case is the same as suggested by the GUM1 approach, the PDF of the length (or width) is equal to the PDF associated to the random uncertainty contribution. Therefore, the possible values of length and width distribute, respectively, according to a uniform PDF centered on values $l_m - e_{sys}^l$ and $w_m - e_{sys}^w$, of width 0.1 mm, where the values of e_{sys}^l and e_{sys}^w are again the ones given in sec. III-B1.

When the RFV approach is followed, the measurement result is directly represented with a random-fuzzy variable (RFV), as shown in previous Sec. II-B. The available metrological information is that only random contributions are present, and that they distribute uniformly over intervals of width 0.1 mm, centered on values $l_m - e_{sys}^l$ and $w_m - e_{sys}^w$, respectively for length and width of the block under test. Therefore, the RFV will have nil internal PD (no systematic contributions) and a triangular random PD, since the probability-possibility transformation of a uniform PDF provides a triangular PD [26]. The mean values of the triangular PDs will be the same as those of the initial PDFs.

Figs. 4 and 5 show the results obtained by the three approaches, when only one caliper and two different calipers are used, respectively. The comparison is performed in terms of possibility distributions and coverage intervals. This means that, when the MC approach is considered, the obtained PDFs are transformed into the equivalent PDs (by applying the probability-possibility transformation), and when the GUM approach is followed, the obtained intervals are drawn at levels

$\alpha = 1 - p$, so that coverage intervals at the same coverage probability can be immediately compared between the three approaches. In particular: the green lines show the reference values l_{ref} and w_{ref} of length and width; the cyan lines show the RFVs, obtained by applying directly the RFV approach; the blue dashed lines represent the result of the MC approach, converted into a PD; the red lines show two coverage intervals (corresponding to coverage probabilities 95.45% and 68.27%) obtained with the GUM approach. It can be readily checked that the blue dashed lines, representing the MC result in terms of PD, are perfectly superposed to the external cyan PDs of the RFVs representing the measurement results.

According to the above considerations, Figs. 4 and 5 show that all approaches provide the same results in this case, where only random contributions affect the final measurement results. Figs. 4 and 5 also show the residual systematic effect after calibration, due to the different resolution between the employed Vernier calipers and the reference gauge blocks.

B. Case 2A

In this case, since it is not known which specific caliper is used to measure length and width, it is not possible to make a compensation of the systematic errors. Therefore, both random and systematic contributions to uncertainty must be taken into account to provide the final measurement result, with the associated combined uncertainty.

When the GUM approach is followed, the combined uncertainty is obtained by quadratically summing the uncertainties due to the random and systematic contributions [1]:

$$u_c = \sqrt{u_{ran}^2 + u_{sys}^2}$$

having assumed that the contributions are independent. Since the PDFs are assumed to be uniform, it is:

$$u_{ran} = \frac{0.05}{\sqrt{3}} \text{ mm and } u_{sys} = \frac{0.1}{\sqrt{3}} \text{ mm.}$$

Hence, the coverage intervals are obtained as intervals centered on l_m and w_m , with semi-width $k_p \cdot u_c(y)$ [1]. According to the GUM, the k_p values can be obtained by applying the *Central Limit Theorem*. In this case, as an example, the coverage intervals at coverage probabilities 95.45% and 68.27% are obtained when $k_p = 2$ and $k_p = 1$ are taken.

In this simple example of uniform PDFs, however, it is also possible to obtain a better estimate of the coverage intervals in an analytical way, by considering that the sum of two uniform PDFs is a trapezoidal PDF and by evaluating in a strict mathematical way the coverage intervals.

The GUM Supplement 1 follows the same representation of the systematic contributions as the GUM: in the MC simulation, it considers a different realization of the systematic error in each considered trial and, therefore, the same result as the one provided by the GUM is obtained [2]. However, this approach does not represent the actual measurement procedure.

The use of a specific caliper, whose systematic error is represented by a given probability distribution, can be mathematically represented as a single, random selection of that caliper from the whole set of available calipers showing the given probability distribution of the systematic error. When the selected caliper is used in the subsequent measurement operations, its systematic error will affect the measurement result in the same way, though unknown. Therefore, changing the value of this error at every trial representing a new measurement operation, as suggested by [2], does not reflect reality.

On the other hand, since the caliper has been randomly selected from the available set, its systematic error is unknown and, to consider this lack of information and the effect of this random selection, the MC simulation is performed as follows.

- A random realization of the systematic error is considered, kept constant and N (10^7 in the considered numerical example) subsequent realizations of the random error are considered.
- A new random realization of the systematic error is then considered, representing a different possible selection of the caliper, and the above procedure is repeated N times.

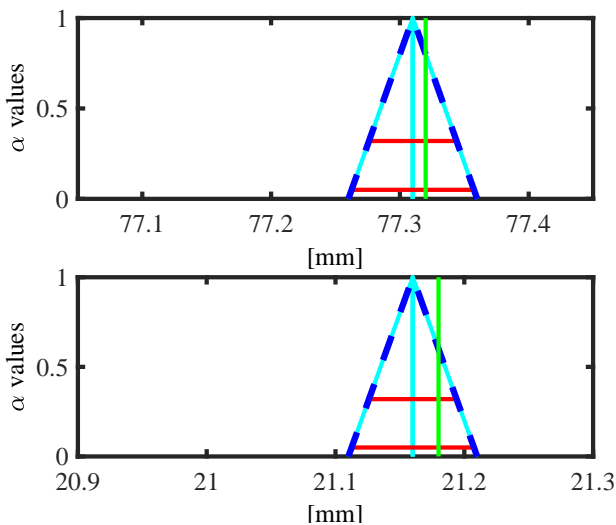


Fig. 4. Results obtained in case 1A, when the same Vernier caliper is used to measure width (lower plot) and length (upper plot) of the block. Green lines: reference values. Red lines: coverage intervals provided by the GUM approach. Blue dashed lines: PDFs obtained from MC approach. Cyan lines: RFVs.

Since the same considerations can be done for both the length and the width measurements, let us focus only on the length, for the sake of brevity.

According to the above considerations, in our experiment, since a single caliper is used to measure the length, in each different Monte Carlo iteration, a unique realization e_{sys}^l of the systematic error shall be considered, while different possible realizations e_{ran_k} of the random errors are considered. Furthermore, since, according to the assumptions in Sec. III-B1, the same caliper is used for both length and width, $e_{sys}^l = e_{sys}^w = e_{sys}$. Then, according to the assumptions in Table I, e_{sys} is one random extraction from a uniform PDF over interval ± 0.1 mm, while each e_{ran_k} value is a random extraction from a uniform PDF over interval ± 0.05 mm.

The possible values of the length are then obtained as:

$$l_k = l_m + e_{sys} + e_{ran_k} \quad (10)$$

where $k = 1 \dots 10^7$, from which a histogram can be built. Since, in (10), l_m is a single number, e_{sys} is a single number and e_{ran_k} are extractions from a uniform PDF over interval ± 0.05 mm, it follows that the obtained histogram is an approximation of a uniform PDF over interval $(l_m + e_{sys}) \pm 0.05$ mm. This PDF, however, refers only to one single caliper, since the same systematic error e_{sys} is considered in (10).

Since also the other calipers could be used, as above discussed, it is necessary to repeat the Monte Carlo simulation (10) $i = 1 \dots 10^7$ times, each time taking a different random realization of the systematic error e_{sys_i} . Each simulation will provide a uniform PDF over interval $(l_m + e_{sys_i}) \pm 0.05$ mm. The whole set of simulations will then provide 10^7 different uniform PDFs, whose modes distribute uniformly over interval $l_m \pm 0.1$ mm. The solution of this case 2A is therefore given by a uniform PDF over interval $l_m \pm 0.15$ mm. This PDF is representative of the possible measured values of the length of the block.

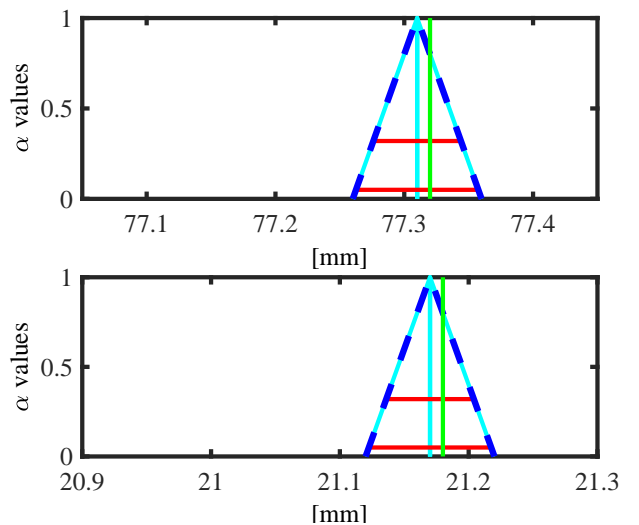


Fig. 5. Results obtained in case 1A, when two Vernier calipers are used to measure width (lower plot) and length (upper plot) of the block. Green lines: reference values. Red lines: coverage intervals provided by the GUM approach. Blue dashed lines: PDFs obtained from MC approach. Cyan lines: RFVs.

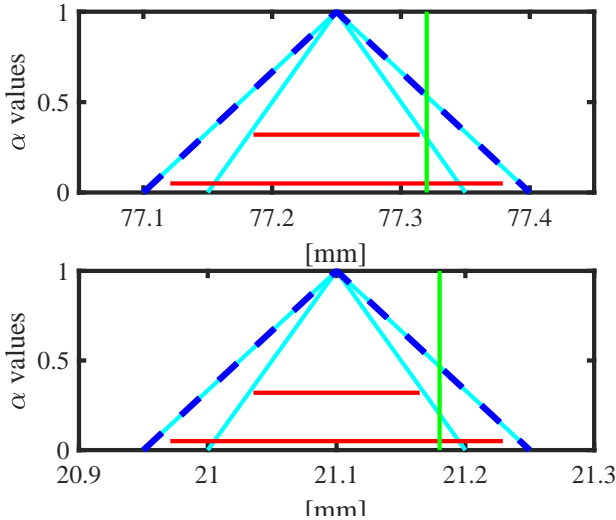


Fig. 6. Result obtained in case 2A. Upper plot: length of the block. Bottom plot: width of the block. Green lines: reference values. Red lines: coverage intervals provided by the GUM approach. Blue dashed lines: PDs obtained from MC approach. Cyan lines: RFVs.

Similarly, when the width is considered, a uniform PDF over interval $w_m \pm 0.15$ mm is obtained.

When the RFV approach is followed, RFVs are directly built for length and width, according to the whole available metrological information. For both width and length of the block, the available metrological information is that the random contributions distribute uniformly over an interval of width 0.1 mm and that the systematic contributions distribute uniformly over an interval of width 0.2 mm. Therefore, according to the probability-possibility transformation [26], a triangular random PD r^{ran} is obtained and a triangular internal PD r^{int} is obtained, so that, combining them according to (4), the whole RFV is obtained. The mean values of the obtained RFVs are l_m and w_m respectively.

Fig. 6 shows the results obtained by the three approaches, represented in terms of PDs and coverage intervals: the meaning of each line is the same as described in the previous case 1A. Since the dashed blue lines representing the MC results in terms of PDs are perfectly superposed to the external cyan PDs of the RFVs representing the measurement results, Fig. 6 clearly shows that the MC and RFV approaches provide the same final results. Moreover, the RFV approach provides more information, since the RFVs clearly show the effects of the random and systematic contributions, separately. On the other hand, the GUM approach underestimates, in this case, the coverage intervals. This is due to the fact that the GUM approach implies some compensation between the two uncertainty contributions.

C. Case 3A

The difference between cases 2A and 3A is that, in case 2A, the available information shows that the contributions distribute over given intervals according to uniform PDFs, while, in case 3A, these PDFs are not known. Since, when a probabilistic approach is followed, when the PDF is not

known, a uniform PDF is generally assumed, it follows that cases 2A and 3A are handled in the same probabilistic way. This is clearly a disadvantage of the probabilistic approach, which is not able to handle two very different situations in a proper way.

On the other hand, when the RFV approach is followed, the difference between cases 2A and 3A can be suitably taken into account. In the possibility domain, the situation in which only an interval is given and nothing else is known about the distribution of values over this interval is called *total ignorance* and is represented by a rectangular PD [26]. It is worth noting that *total ignorance* is very common in industrial applications, since all instrument's data sheets only provide interval of variations, without any further information. Hence, according to all available information, the RFVs shown in cyan lines in Fig. 7 are obtained. The figure clearly shows how the probabilistic approaches underestimate the coverage intervals in this situation (the meaning of each line is the same as described in previous case 1A).

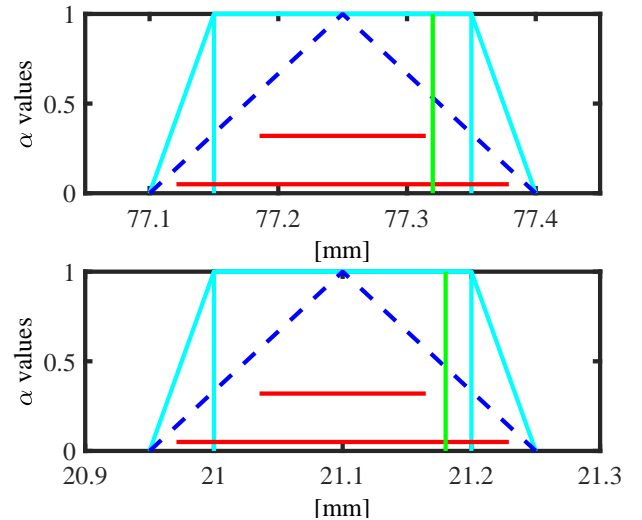


Fig. 7. Result obtained in case 3A. Upper plot: length of the block. Bottom plot: width of the block. Red lines: coverage intervals provided by the GUM approach. Blue dashed lines: PDs obtained from MC approach. Cyan lines: RFVs.

D. Case A conclusions

By comparing the RFV in this Fig. 7 with the RFVs in Figs. 4, 5 and 6, it can be noted that the same supports⁴ S_l and S_w of the RFVs is obtained in case 2A and 3A, while smaller supports are obtained in case 1A. This is coherent with the fact that, in case 1A, the systematic effect has been compensated.

Figs. 4-7 also show that the coverage intervals increase from case 1A to case 3A, coherently to the fact that the available metrological information decreases.

V. CASE B RESULTS

In Case B, the area of the block is evaluated, according to the measured values considered in previous case A.

⁴The support of an RFV is defined as the α -cut for $\alpha = 0$

A. Case 1B

In case 1B, the employed calipers (one or two) are known and the systematic error affecting the measurements of length and width can be compensated for. Therefore, only random contributions affect the final measurement uncertainty.

When the GUM approach is followed, the uncertainty associated to the measured area A_m is obtained by applying the LPU for uncorrelated quantities, since the two measurement procedures are independent from each other:

$$u_{A_m} = \sqrt{\left(\frac{\partial f}{\partial l}\right)^2 \cdot u_l^2 + \left(\frac{\partial f}{\partial w}\right)^2 \cdot u_w^2}$$

Since $u_l = u_w = u_{ran}$, it follows:

$$u_{A_m} = \sqrt{\left[(w_m - e_{sys}^w)^2 + (l_m - e_{sys}^l)^2\right] \cdot u_{ran}^2} \quad (11)$$

Then, the coverage intervals are obtained as intervals centered on $(l_m - e_{sys}^l) \cdot (w_m - e_{sys}^w)$, with semi-width $k_p \cdot u_{A_m}$ [1]. Of course, when the same caliper is used to measure length and width, $e_{sys}^l = e_{sys}^w$ and, when two calipers are used, $e_{sys}^l \neq e_{sys}^w$, according to the assumptions in Sec. III-B2. According to the GUM, the k_p values can be obtained by applying the *Central Limit Theorem*. Under this assumption, the confidence interval at coverage probabilities 95.45% and 68.27% are obtained when $k_p = 2$ and $k_p = 1$ are applied.

When the MC approach is followed, the possible values of the area are obtained as:

$$A_k = \left(l_m - e_{sys}^l + e_{ran_k}^{(1)}\right) \cdot \left(w_m - e_{sys}^w + e_{ran_k}^{(2)}\right) \quad (12)$$

where $e_{ran_k}^{(1)}$ and $e_{ran_k}^{(2)}$ are two random extractions from the uniform PDF representing the random contributions to uncertainty and $k = 1 \dots 10^7$. It is $e_{sys}^l = e_{sys}^w$ if the same caliper is used to measure length and width, while it is $e_{sys}^l \neq e_{sys}^w$ if two different calipers are used, with the values assumed in Sec. III-B2. The two obtained histograms approximate two PDFs, which represent the expected distribution of the values that can be attributed to the values of the area, in the two different considered situations. These PDFs can be then converted into equivalent PDs, according to the probability-possibility transformation [26].

When the RFV approach is followed, length and width are represented by the two RFVs (cyan lines) in Figs. 4 or 5, when the same caliper or two calipers are used, respectively. To correctly multiply the two RFVs and obtain the RFV associated to A_m , it is necessary to correctly consider all the available metrological information: only random contributions which affect the measurements of length and width independently are considered. Therefore, according to the considerations done in Sec. II-B, the t -norm T_{prod} is applied to the triangular random PDs, considering a correlation factor $\rho = 0$ [5], [7].

Figs. 8 and 9 show the results obtained with the three different approaches, when the same Vernier caliper or two different calipers are employed, respectively (the meaning of the lines is the same as described for case 1A). They clearly show that the RFV and MC approaches provide the same results. On the other hand, the coverage intervals provided by the GUM approach are different from the corresponding

coverage intervals provided by the MC and RFV approaches at the same coverage probabilities. In particular, in this case, greater coverage intervals are obtained at higher coverage probabilities, while narrower coverage intervals are obtained at lower coverage probabilities. This shows the theoretical limitation of the GUM approach. In fact, when the PDF of the measurement result is not known (as it generally happens with the GUM approach, which only propagates standard deviations), it is not possible to correctly evaluate the coverage probabilities associated to given coverage intervals (or vice-versa), and only approximations can be made, by applying the *Central Limit Theorem*. It is also worth noting that, in some particular practical cases, like this one, the final PDF can be also analytically obtained, so that the correct coverage probability can be assigned to the intervals obtained from the combined standard uncertainty.

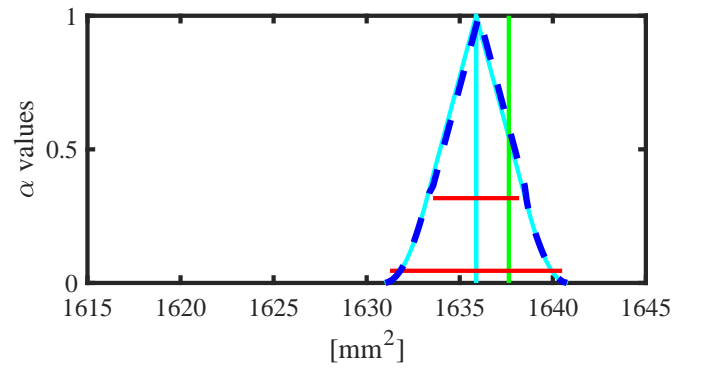


Fig. 8. Result obtained in case 1B, when the same Vernier caliper is used to measure width and length of the block. Green line: area reference value. Red lines: coverage intervals provided by the GUM approach. Blue dashed lines: PD obtained from MC approach. Cyan lines: RFV.

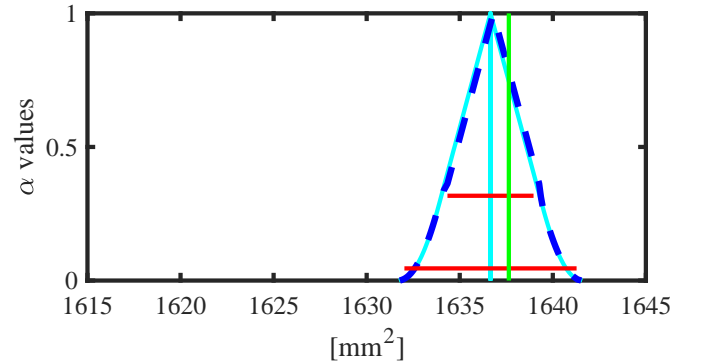


Fig. 9. Result obtained in case 1B, when two Vernier calipers are used to measure width and length of the block. Green line: area reference value. Red lines: coverage intervals provided by the GUM approach. Blue dashed lines: PD obtained from MC approach. Cyan lines: RFV.

B. Case 2B

In case 2B, one caliper is chosen randomly and it is not possible to compensate for the systematic error it introduces, since it is not known. It follows that both the measurements of length and width are affected by both random and systematic contributions to uncertainty.

However, the knowledge that the two measurements are taken with the same caliper allows us to state that, even if its value is unknown, the two measurements are affected by the same systematic error. This metrological information should be of course taken into account when combining uncertainties.

When the GUM approach is followed, the above information can be used to set a correlation factor $\rho = 1$ between the systematic contributions; conversely, a correlation factor $\rho = 0$ is considered between the random contributions. The uncertainty u_{A_m} affecting A_m is obtained by [1]:

$$u_{A_m} = \sqrt{u_{A_{ran}}^2 + u_{A_{sys}}^2} \quad (13)$$

where, according to the above considerations, $u_{A_{ran}}$ and $u_{A_{sys}}$ are given by:

$$u_{A_{ran}} = \sqrt{(w_m^2 + l_m^2) \cdot u_{ran}^2} \quad (14)$$

$$u_{A_{sys}} = \sqrt{(w_m^2 + l_m^2 + 2 \cdot l_m \cdot w_m) \cdot u_{sys}^2} \quad (15)$$

Hence, the coverage intervals are obtained as intervals centered on A_m with semi-width $k_p u_{A_m}$ [1]. According to the GUM, the k_p values can be obtained by applying the *Central Limit Theorem*. Under this assumption, the coverage interval at coverage probabilities 95.45% and 68.27% are obtained when $k_p = 2$ and $k_p = 1$ are applied.

When the MC approach is followed, according to the considerations already reported for case 2A, the following Monte Carlo simulation can be performed:

$$A_k = (l_m + e_{sys} + e_{ran_k}^{(1)}) \cdot (w_m + e_{sys} + e_{ran_k}^{(2)}) \quad (16)$$

where $k = 1 \dots 10^7$. $e_{ran_k}^{(1)}$ and $e_{ran_k}^{(2)}$ are two random extractions from the PDF representing the distribution of the random contributions, while e_{sys} is a single random extraction from the PDF representing the distribution of the possible systematic errors. The same extraction e_{sys} applies to both measurements because, according to Table II, a single caliper is used in this case 2B and $e_{sys}^l = e_{sys}^w = e_{sys}$. Moreover, the same extraction e_{sys} applies to every run k , since one specific caliper always affects the measured values with the same systematic error.

When a generic caliper is considered, (16) provides the red histogram shown in Fig. 10. Since also the other calipers could be used, it is necessary to repeat the Monte Carlo simulation (16) $i = 1 \dots 10^7$ times, each time taking a different random extraction e_{sys_i} . These simulations provide histograms with a similar shape as the red one in Fig. 10, centered on different values $(l_m + e_{sys_i}) \cdot (w_m + e_{sys_i})$. In particular, in Fig. 10, the lowest and the highest of all obtainable histograms are reported⁵ (green and violet histograms respectively). The final solution of the MC approach is therefore given by the whole family of the obtainable histograms. The orange line in Fig. 10 shows the boundary of this family. From this curve, by applying the normalization condition for probability distributions, the final result given by the MC approach in terms

⁵The lowest and the highest of all obtainable histograms are obtained, for case 2B, by setting, in (16), the minimum and the maximum possible values, respectively, for e_{sys} (i. e. $e_{sys} = -0.1$ mm for the lowest histogram; $e_{sys} = 0.1$ mm for the highest histogram).

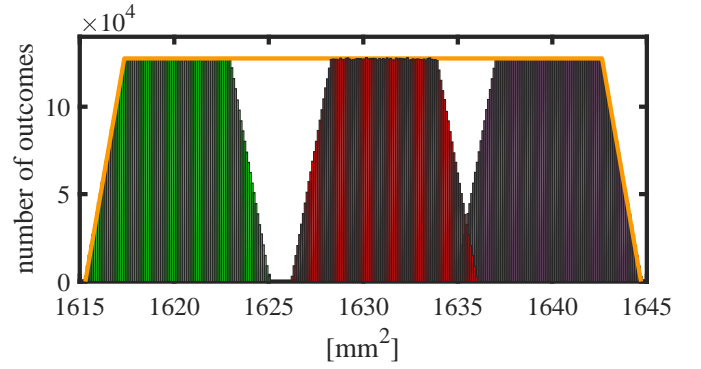


Fig. 10. A generic (in red color), the lowest (in green color) and the highest (in violet color) histograms obtained with the Monte Carlo simulation expressed by (16). The orange line shows the boundary of all the obtainable histograms and represents the final solution of the MC approach in case 2B.

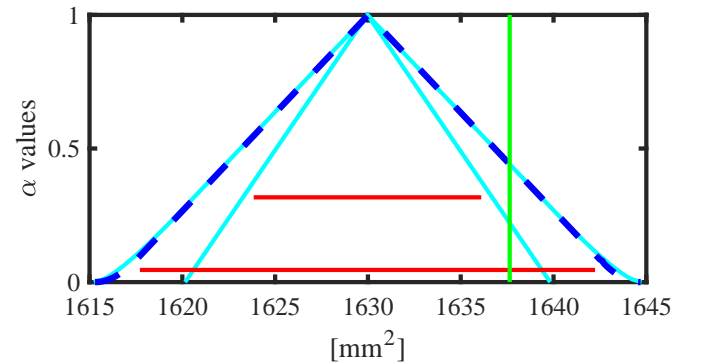


Fig. 11. Result obtained in case 2B. Green line: area reference value. Red lines: coverage intervals provided by the GUM approach. Blue dashed lines: PD obtained from MC approach. Cyan lines: RFV.

of a PDF is obtained. This PDF can be then converted into the corresponding PD by applying the probability-possibility transformation [26].

When the RFV approach is followed, the RFVs of length and width are the RFVs of Fig. 6 (cyan lines). In order to obtain the RFV associated to A_m , according to the above considerations, t -norm T_{prod} is applied to the random PDs and $\rho = 0$ is considered; t -norm T_{min} is applied to the internal PDs and $\rho = 1$ is considered. The closed-form equations derived in [5], [7] are employed to get the desired PDs.

Fig. 11 shows the results obtained with the three different approaches. The meaning of the lines is the same as described for case 1A.

Fig. 11 shows that very similar results are obtained when the MC and RFV approaches are followed, since the blue dashed PD representing the result of the MC simulations is almost totally overlapping the external PD of the obtained cyan RFV. On the other hand, the GUM approach provides, in this case, narrower coverage intervals and this is mainly due to the fact that, because of (13), the systematic and random uncertainties compensate with each other.

It is the Author's opinion that this compensation is not metrologically correct, and this is proved by the results obtained following the RFV and the Monte Carlo approaches, which both have correctly considered the non-random impact of the

systematic contribution on the measurement procedure.

C. Case 3B

In case 3B, the same PDFs are associated to the random and systematic contributions, as in case 2B, but length and width are measured with two different calipers. Under this new assumption, even if the systematic errors introduced by the two calipers are unknown, it is possible to state that they are surely different and independent of each other. This different metrological information is taken into account when combining uncertainties, by considering a correlation factor $\rho = 0$ also between the systematic contributions. Hence, the following applies.

When the GUM approach is followed, u_{A_m} is still given by (13), where $u_{A_{ran}}$ is still given by (14), while $u_{A_{sys}}$ is now given by:

$$u_{A_{sys}} = \sqrt{(w_m^2 + l_m^2) \cdot u_{sys}^2} \quad (17)$$

Hence, the coverage intervals are obtained as intervals centered on A_m with semi-width $k_p u_{A_m}$ [1]. According to the GUM, the k_p values can be obtained by applying the *Central Limit Theorem*. Under this assumption, the confidence interval at coverage probabilities 95.45% and 68.27% are obtained when $k_p = 2$ and $k_p = 1$ are applied.

When the MC approach is followed, according to the same considerations as in the previous cases, the following Monte Carlo simulation can be performed:

$$A_k = \left(l_m + e_{sys}^{(1)} + e_{ran_k}^{(1)} \right) \cdot \left(w_m + e_{sys}^{(2)} + e_{ran_k}^{(2)} \right) \quad (18)$$

where where $k = 1 \dots 10^7$. $e_{ran_k}^{(1)}$ and $e_{ran_k}^{(2)}$ are two random extractions from the PDF representing the random contributions, while $e_{sys}^{(1)}$ and $e_{sys}^{(2)}$ are two random extractions from the PDF representing the distribution of the possible systematic errors. Two different extractions now are taken, since two calipers are used, according to Table II. Moreover, as long as the same calipers are supposed to be employed in the Monte Carlo simulations, the measured values are affected by the same systematic error, and therefore no different extractions are taken for the different runs k .

The histogram obtained from (18) (red colour in Fig. 12) is representative of one possible pair of calipers. Since also other pairs could be randomly chosen, it is necessary to repeat the Monte Carlo simulations $i = 1 \dots 10^7$ times, each time taking two different random extractions $e_{sys_i}^{(1)}$ and $e_{sys_i}^{(2)}$. The green and violet histograms in Fig. 12 represent the lowest and highest of all obtainable histograms⁶. Similarly to Case 2B, from the orange line in Fig. 12, which envelopes all obtainable histograms, it is possible to build the PDF associated to the area value, according to the Monte Carlo simulations. Furthermore, by applying the probability-possibility transformation [26], a corresponding PD is obtained.

⁶In case 3B, the lowest of all obtainable histograms is obtained by setting, in (18), $e_{sys}^{(1)} = -0.1$ mm and $e_{sys}^{(2)} = e_{sys}^{(1)} + 0.01$ mm. In fact, the two calipers must introduce, in this case, the lowest possible values of the systematic errors. Since two different calipers are employed, they cannot assume the same value of the systematic error. Therefore, a difference of 0.01 mm is considered, which corresponds to the Johansson gauge blocks accuracy (which are used to calibrate the calipers themselves). Similarly, the highest histogram is obtained by setting $e_{sys}^{(1)} = 0.1$ mm and $e_{sys}^{(2)} = e_{sys}^{(1)} - 0.01$ mm.

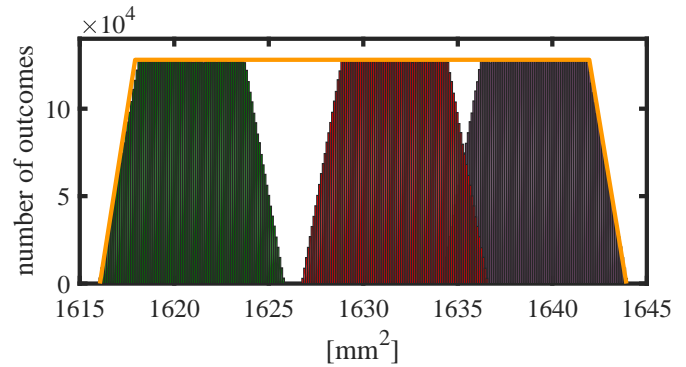


Fig. 12. A generic (in red color), the lowest (in green color) and the highest (in violet color) histograms obtained with the Monte Carlo simulations expressed by (18). The orange line shows the boundary of all the obtainable histograms and represents the final solution of the MC approach in case 3B.

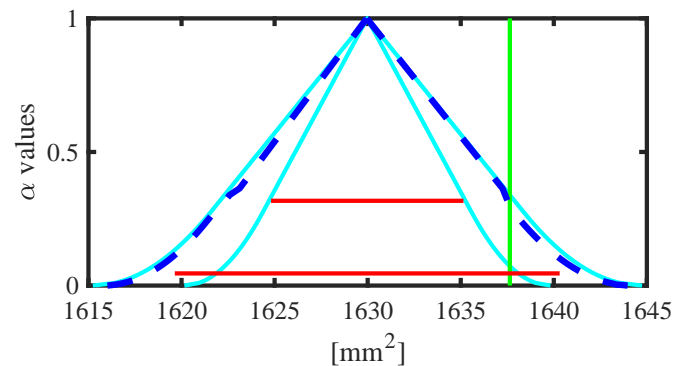


Fig. 13. Result obtained in case 3B. Green line: area reference value. Red lines: coverage intervals provided by the GUM approach. Blue dashed lines: PD obtained from MC approach. Cyan lines: RFV.

When the RFV approach is followed, the RFVs of the length and width are the ones in Fig. 6. However, with respect to previous case 2B, the different metrological information imposes to choose different t -norms to be applied. In particular, for both the random and internal PDs, t -norm T_{prod} is applied and a correlation factor $\rho = 0$ is considered [5], [7].

Fig. 13 shows the obtained results with the three different approaches (the meaning of the lines is the same as described for case 1A). This figure allows to draw similar considerations as those drawn at the end of case 2B.

D. Case 4B

In case 4B, one single caliper is used to measure length and width, as well as in previous case 2B. However, in this case, the available metrological information changes: no PDF is associated to the distribution of the possible systematic errors and only an interval of variation is given, while the same uniform PDF is associated to the random contributions affecting the measurement procedure.

As already discussed for previous case 3A, the probabilistic (GUM and MC) approaches cannot distinguish the two situations in which a uniform PDF is given and only an interval is given but no PDF (*total ignorance*). Hence, case 4B falls in case 2B, as far as these two approaches are concerned.

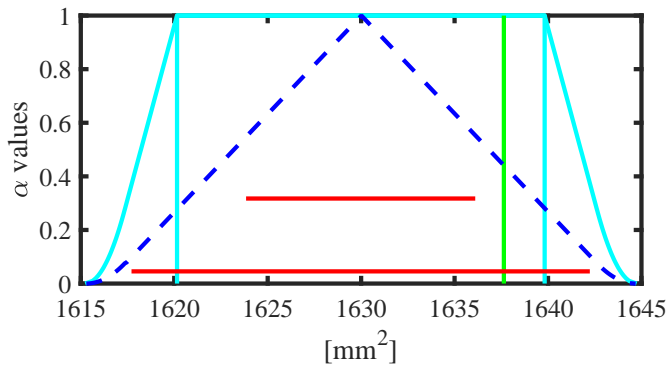


Fig. 14. Result obtained in case 4B. Red lines: coverage intervals provided by the GUM approach. Blue dashed lines: PD obtained from MC approach. Cyan lines: RFV.

On the other hand, when the RFV approach is followed, the different metrological information of this case 4B is transferred into the different shape of the RFVs, as shown in Fig. 7. To obtain the RFV of A_m , according to the the same considerations as in case 2B, t -norm T_{prod} is applied to the random PDs and $\rho = 0$ is considered; t -norm T_{min} is applied to the internal PDs and $\rho = 1$ is considered [5], [7]. This leads to the RFV shown in cyan lines in Fig. 14. In this figure, the red and dashed blue lines report the GUM and MC results, as evaluated for case 2B. As expected, since the probabilistic approaches cannot consider total ignorance in the correct mathematical way, they provide narrower coverage intervals than the RFV approach.

E. Case 5B

In case 5B, two calipers are used to measure length and width, as in previous case 3B. However, in this case, the available metrological information changes: no PDF is associated to the distribution of the possible systematic errors and only an interval of variation is given, while the same uniform PDF is associated to the random contributions affecting the measurement procedure.

According to the considerations done for previous case 4B, the GUM and MC approaches cannot distinguish cases 3B and 5B. On the other hand, when the RFV approach is followed, the RFVs of width and length are the ones in Fig. 7. To obtain the RFV of A_m , according to the same assumptions as in case 3B, for both the random and internal PDs, t -norm T_{prod} is applied and a correlation factor $\rho = 0$ is considered [5], [7]. This leads⁷ to the RFV in cyan lines in Fig. 15. The results obtained with the GUM and MC approaches are also reported (as obtained in case 3B) for a more immediate comparison. Since the probabilistic approaches cannot consider total ignorance in the correct mathematical way, they provide narrower coverage intervals than the RFV approach.

⁷It can be noted that the RFV in Fig. 15 is equal to the RFV in Fig. 14. This is due to the fact that the internal PDs of the RFVs of width and length are rectangular. In fact, when rectangular PDs are combined, the application of whichever t -norm always provides the same result. However, this is only a particular situation and not a general rule, as also proved by the RFVs in Figs. 11 and 13.

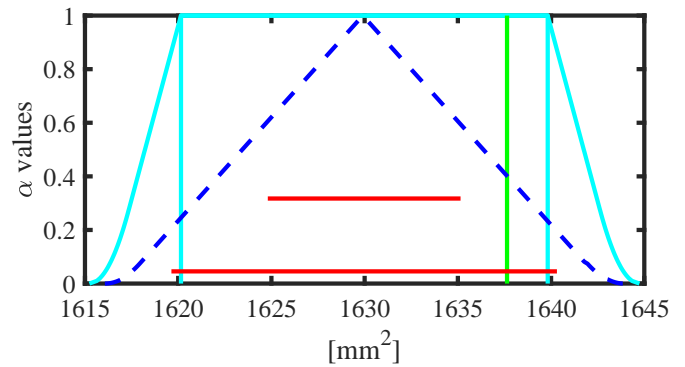


Fig. 15. Result obtained in case 5B. Red lines: coverage intervals provided by the GUM approach. Blue dashed lines: PD obtained from MC approach. Cyan lines: RFV.

F. Case B conclusions

By comparing Figs. 8, 9, 11, 13-15, same considerations as the ones reported for case A can be drawn.

VI. CONCLUSIONS

This paper has shown how the possibilistic approach to measurement uncertainty can always consider, represent and propagate, in a correct mathematical way, all available metrological information.

Different sets of possible relevant metrological information have been considered and discussed through simple examples of typical measurement situations. It has been proved that the available information must be correctly employed to identify the most suitable way to represent and combine the measurement results, and to represent the different contributions to uncertainty, no matter on the approach followed to evaluate uncertainty.

The paper has proved that the same measurement results and uncertainty contributions, although represented by the same variables (PDFs or RFVs), must be processed in different ways, according to the available information on the way the uncertainty contributions originated and/or interact.

Three different approaches (GUM, MC and RFV) have been applied and the obtained results compared. The obtained results are summarized in Table III, where the X symbol does not forcefully mean that the provided result is totally incorrect, but only that the considered method refers to a mathematical approach [26], [29] that is not theoretically capable of handling the available information, even in those cases where the provided numerical results approximate, often by chance, the correct one.

Table III shows that only the RFV approach can handle all considered metrological situations. This is a direct consequence of being based on a mathematical theory which is more general than the probability theory [26], [29]. In particular, it can be stated that, when there is full knowledge of the PDFs associated to all uncertainty contributions, the Monte Carlo simulations and the RFV approach provide the same results. Hence, in this case, both approaches can be applied. The RFV approach, however, has also the advantage to be faster in the implementation, since it does always refer to closed-form

TABLE III
COMPARISON OF THE THREE APPROACHES.

case	GUM	MC	RFV
1A	OK	OK	OK
2A	X	OK	OK
3A	X	X	OK
1B	X	OK	OK
2B	X	OK	OK
3B	X	OK	OK
4B	X	X	OK
5B	X	X	OK

algebraic formulas, and provide additional information about the final measurement result, with respect to Monte Carlo. In fact, as shown in Figs. 4-6 and 8-13, the Monte Carlo simulations are able to provide only the external PD of the final RFV. This means that only the overall uncertainty is obtained, while the RFV approach provides information on the effect of each single contribution (the random and the systematic ones) to the final measurement result.

On the other hand, only the RFV approach is able, according to the mathematical theory of possibility [26], [29] to consider also situations of poor knowledge, where not all PDFs are known (total ignorance), as shown in Figs. 7, 14 and 15. This capability is very useful in the industrial field, where the majority of the measurement procedures are characterized by poor knowledge.

This paper considered a few, simple and didactic examples to give evidence of the above statement in simple cases, easily understandable. Of course, the simplest the examples, the weakest the reasons supporting an approach might appear. However, several applications of the RFV approach in different and definitely more complex situations have been published [34]–[36], proving that this approach provides solutions otherwise not satisfactory.

REFERENCES

- [1] JCGM 100:2008, *Evaluation of Measurement Data – Guide to the Expression of Uncertainty in Measurement, (GUM 1995 with minor corrections)*, Joint Committee for Guides in Metrology, 2008. [Online]. Available: <http://www.bipm.org/en/publications/guides/gum.html>
- [2] JCGM 101:2008, *Evaluation of measurement data – Supplement 1 to the Guide to the expression of uncertainty in measurement – Propagation of distributions using a Monte Carlo method*, Joint Committee for Guides in Metrology, 2008. [Online]. Available: <http://www.bipm.org/en/publications/guides/gum.html>
- [3] A. Ferrero, M. Prioli, and S. Salicone, “Joint random-fuzzy variables: A tool for propagating uncertainty through nonlinear measurement functions,” *IEEE Trans. Instrum. Meas.*, vol. 65, no. 5, pp. 1015–1021, May 2016.
- [4] A. Ferrero, M. Prioli, and S. Salicone, “Conditional random-fuzzy variables representing measurement results,” *IEEE Trans. Instrum. Meas.*, vol. 64, no. 5, 2015.
- [5] A. Ferrero, M. Prioli, and S. Salicone, “The construction of joint possibility distributions of random contributions to uncertainty,” *IEEE Trans. Instrum. Meas.*, vol. 63, no. 1, pp. 80–88, 2014.
- [6] A. Ferrero, M. Prioli, S. Salicone, and B. Vantaggi, “A 2-D metrology-sound probability-possibility transformation,” *IEEE Trans. Instrum. Meas.*, vol. 62, no. 5, pp. 982–990, 2013.
- [7] A. Ferrero, M. Prioli, and S. Salicone, “Processing dependent systematic contributions to measurement uncertainty,” *IEEE Trans. Instrum. Meas.*, vol. 62, no. 4, pp. 720–731, 2013.
- [8] G. Mauris, “A review of relationships between possibility and probability representations of uncertainty in measurement,” *IEEE Trans. Instrum. Meas.*, vol. 62, no. 3, pp. 622–632, 2013.
- [9] A. Ferrero and S. Salicone, “Uncertainty: Only one mathematical approach to its evaluation and expression?” *IEEE Trans. Instrum. Meas.*, vol. 61, no. 8, pp. 2167–2178, 2012.
- [10] A. Ferrero and S. Salicone, “The construction of random-fuzzy variables from the available relevant metrological information,” *IEEE Trans. Instrum. Meas.*, vol. 58, no. 2, pp. 365–374, 2009.
- [11] G. Mauris, “Representing and approximating symmetric and asymmetric probability coverage intervals by possibility distributions,” *IEEE Trans. Instrum. Meas.*, vol. 58, no. 1, pp. 41–45, 2009.
- [12] A. Ferrero and S. Salicone, “An original fuzzy method for the comparison of measurement results represented as random-fuzzy variables,” *IEEE Trans. Instrum. Meas.*, vol. 56, no. 4, pp. 1292–1299, 2007.
- [13] A. Ferrero and S. Salicone, “Modeling and processing measurement uncertainty within the theory of evidence: Mathematics of random-fuzzy variables,” *IEEE Trans. Instrum. Meas.*, vol. 56, no. 3, pp. 704–716, 2007.
- [14] G. Mauris, “Expression of measurement uncertainty in a very limited knowledge context: A possibility theory-based approach,” *IEEE Trans. Instrum. Meas.*, vol. 56, no. 3, pp. 731–735, 2007.
- [15] A. Ferrero and S. Salicone, “Fully-comprehensive mathematical approach to the expression of uncertainty in measurement,” *IEEE Trans. Instrum. Meas.*, vol. 55, no. 3, pp. 706–712, 2006.
- [16] A. Ferrero and S. Salicone, “A comparative analysis of the statistical and random-fuzzy approaches in the expression of uncertainty in measurement,” *IEEE Trans. Instrum. Meas.*, vol. 54, no. 4, pp. 1475–1481, 2005.
- [17] A. Ferrero and S. Salicone, “The use of random-fuzzy variables for the implementation of decision rules in the presence of measurement uncertainty,” *IEEE Trans. Instrum. Meas.*, vol. 54, no. 4, pp. 1482 – 1488, 2005.
- [18] A. Ferrero and S. Salicone, “The random-fuzzy variables: a new approach for the expression of uncertainty in measurement,” *IEEE Trans. Instrum. Meas.*, vol. 53, no. 5, pp. 1370–1377, 2004.
- [19] G. Mauris, V. Lasserre, and L. Foulloy, “A fuzzy approach for the expression of uncertainty in measurement,” *Measurement*, vol. 29, pp. 165–177, 2001.
- [20] G. Mauris, L. Berrah, L. Foulloy, and A. Haurat, “Fuzzy handling of measurement errors in instrumentation,” *IEEE Trans. Instrum. Meas.*, vol. 49, no. 1, pp. 89–93, 2000.
- [21] M. Grabe, “Estimation of measurement uncertainties - an alternative to the iso guide,” *Metrologia*, vol. 38, no. 2, pp. 97–106, 2001. [Online]. Available: <http://stacks.iop.org/0026-1394/38/i=2/a=1>
- [22] I. Lira, A. Chunovkina, C. Elster, and W. Wger, “Analysis of key comparisons incorporating knowledge about bias,” *IEEE Trans. Instrum. Meas.*, vol. 61, no. 8, pp. 2079–2084, 2012.
- [23] I. Lira and D. Grientschnig, “Deriving pdfs for interrelated quantities: What to do if there is more than enough information?” *IEEE Trans. Instrum. Meas.*, vol. 63, no. 8, pp. 1937–1946, 2014.
- [24] F. Attivissimo, A. Cataldo, L. Fabbiano, and N. Giaquinto, “Systematic errors and measurement uncertainty: An experimental approach,” *Measurement*, no. 4, pp. 1781–1789, 2011.
- [25] G. J. Klir and B. Yuan, *Fuzzy sets and fuzzy logic. Theory and applications*. Englewood Cliffs, NJ, USA: Prentice Hall PTR, 1995.
- [26] S. Salicone, *Measurement Uncertainty: an approach via the mathematical theory of evidence*, ser. Springer series in reliability engineering. New York, NY, USA: Springer, 2007.
- [27] A. Ferrero, M. Prioli, and S. Salicone, “Uncertainty propagation through non-linear measurement functions by means of joint random-fuzzy variables,” in *I2MTC 2015*, Pisa, Italy, May 11–14, 2015.
- [28] D. Dubois, L. Foulloy, G. Mauris, and H. Prade, “Probability-possibility transformations, triangular fuzzy sets, and probabilistic inequalities,” *Reliable Computing. Kluwer Academic Publishers*, vol. 10, pp. 273–297, 2004.
- [29] G. Shafer, *A Mathematical Theory of Evidence*. Princeton, NJ, USA: Princeton Univ. Press, 1976.
- [30] C. Alsina, M. J. Frank, and B. Schweizer, *Associative Functions: Triangular Norms and Copulas*. World Scientific, 2006.
- [31] L. A. Zadeh, “Fuzzy sets as a basis for a theory of possibility,” *Fuzzy Sets and Systems*, vol. 1, no. 1, pp. 3–28, 1978.
- [32] E. P. Klement, R. Mesiar, and E. Pap, *Triangular Norms*. Dordrecht, Netherlands: Kluwer, 2000.
- [33] A. Ferrero, M. Prioli, S. Salicone, and W. Jiang, *Combination of measurement uncertainty contributions via the generalized Dombi operator*. Atlantis Press, 2015, pp. 1507–1513.
- [34] Q. Zhu, Z. Jiang, Z. Zhao, and H. Wang, “Uncertainty estimation in measurement of micromechanical properties using random-fuzzy variables,” *Review of Scientific Instruments*, vol. 77, no. 035107, 2006.

- [35] M. Pertile and M. De Cecco, "Uncertainty evaluation for complex propagation models by means of the theory of evidence," *MEASUREMENT SCIENCE AND TECHNOLOGY*, vol. 19, pp. 1–10, 2008.
- [36] Y. Chen and K. A. Hoo, "Uncertainty propagation for effective reduced-order model generation," *Computers and Chemical Engineering*, vol. 34, p. 15971605, 2010.